New Fuel Pin Axial Expansion Reactivity Feedback Model in MARS-LMR

Chiwoong CHOI [a*], and Kwiseok Ha [a]
[a]*Korea Atomic Energy Research Institute(KAERI), 989-111, Daedeok-Daero, Yuseong-Gu, Daejeon, Korea*

[*]*Corresponding author: cwchoi@kaeri.re.kr*

1. Introduction

The Anticipated Transient without Scram (ATWS) events, classified into the design extended condition (DEC), in an event classification for the Prototype Gen-IV sodium cooled Fast reactor (PGSFR) are analyzed with MARS-LMR code. Unprotected Transient Over Power, (UTOP), Unprotected Loss Of Flow (ULOF), and Unprotected Loss Of Heat Sink (ULOHS) are selected as ATWS events. Among these accidents, the ULOF event shows the lowest clad temperature. However, the ULOHS event showed the highest peak clad temperature, due to the positive CRDL/RV expansion reactivity feedback and insufficient DHRS capacity.

In this study, the sensitivity tests are conducted. In the case of the UTOP event, a sensitivity test for the reactivity insertion amount and rate were conducted. This analysis can give a requirement for margin of control rod stop system (CRSS). For example, the CRSS in the PRISM designed based on the 0.4 $ reactivity insertion, which is analyzed with safety analysis of UTOP event [1]. Moreover, the sensitivity tests for weighting factor in the core radial expansion reactivity feedback model were also carried out for all ATWS events. Currently, the reactivity feedback model for the PGSFR is not validated yet. However, the reactivity feedback models in the MARS-LMR are validating with various plant-based data including EBR-II SHRT [2].

2. Models for unprotected events

The MARS-LMR code simulates a multiple heat transport system module and its associated controllers. Fig. 1 shows a plant schematic of the major components of the PGSFR. A primary heat transport system (PHTS) is represented with the reactor vessel flow passages, the primary pump, and the shell side of the IHX. An intermediate heat transport system (IHTS) is represented with the tube side of the IHX, piping, the shell side of the SG, and the intermediate pump.

2.1 Core TH models

The PGSFR core configuration is shown in Figure 2. The MARS-LMR core region is divided into four parallel channels. Each channel is modeled to represent the inner, outer core, hot SA, and non-fuel, respectively. A control rod, reflector, and shield subassemblies are

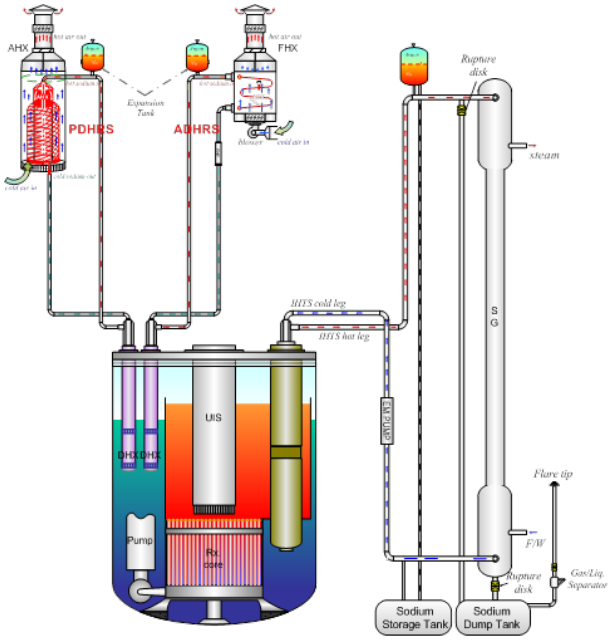

Fig. 1. Schematic of the PGSFR

modeled with averaged non-fuel subassemblies since the power of these non-fuel SAs are small. Usually, an averaged pin within a subassembly is modeled, but a hot subassembly including a hot pin is modeled separately to evaluate safety limit parameters including a maximum clad temperature, and cumulative damage function (CDF). The hot SA is selected as the highest power-to-flow ratio. A peaking factor of 1.2 is multiplied to the averaged power in the hot pin.

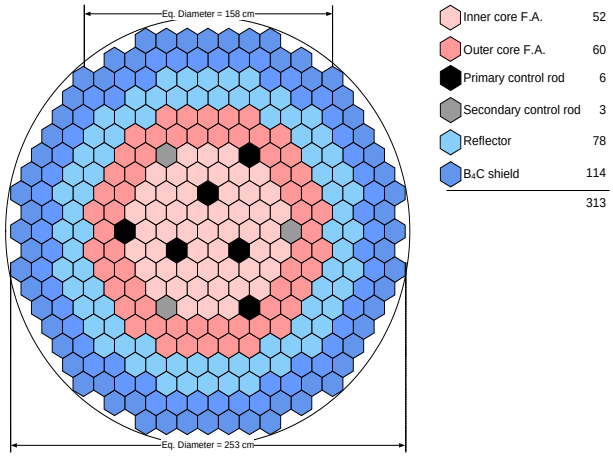

Fig. 2. Core Configuration of the PGSFR

2.2 PHTS Models

Major components of the PHTS (Primary Heat Transport System) are submerged in the sodium pool in the PGSFR. As shown in Fig. 1, both the hot and cold pools have free surfaces and there is a direct mixing of coolant within each of these open pools prior to entering the next component. Therefore, at least two different flows would have to be modeled to characterize the coolant dynamics of the primary system. There are two primary mechanical pumps to drive core coolant. Therefore, the flow from the pump to the core inlet plenum is determined from the pump head and pressure losses in each circuit. Based on dissipation heat from the primary pump and the halving time, which would be key parameters for the analysis of ULOF event.

Four intermediate heat exchangers (IHXs) are installed in the hot pool. And two IHXs are merged and connected to a steam generator as shown in Fig. 1. The IHX has the shell and tube type heat exchanger. The primary hot sodium comes into the shell side inlet and the cold sodium from the SG flows through the down-comer and splits into straight tubes. The IHX flow is determined from the level difference between the two pools, the pressure losses, and the static head in the IHX.

Four decay heat exchangers (DHXs) are located in the cold pool, which is connected to four Decay heat removal systems (DHRSs), respectively as shown in Fig. 1. Relatively hot sodium from the cold pool flows into the shell side inlet and cold sodium from the DHRS flows through the down-comer and divided to the straight tubes. In normal operation, the flow rate is small by slightly opening a damper in each DHRS in order to avoid the solidification in the primary sodium pool. The DHRS is activated with an operational logic when an accident occurred.

The reactor vessel contains basically the entire inventory of the primary sodium coolant in the pool-type design. A vertical wall, called a reactor baffle, divides the primary pool into the hot and cold pools, as shown in Fig. 1.

2.3 IHTS Models

Fig. 3 shows the heat balance during 100% power normal operation, most of heat is removed through the IHXs and SGs, so called as IHTS. The major function of IHTS is a separation between the SG system and PHTS, to protect the influence from accident in SG, such as sodium water reaction (SWR). The two of four IHXs are connected to a single SG, thus, there are two IHTS loops. Each loop has one EM-pump, which is individually modeled with a mechanical pump having a zero coast-down in the MARS-LMR due to the characteristics of EM pump. The SG has single walled straight tubes, which is appropriately modeled with a weighted single tube heat structure. And expansion tank will be integrated in the hot-leg of the IHTS, however, it is not modeled in this analysis because it is under-

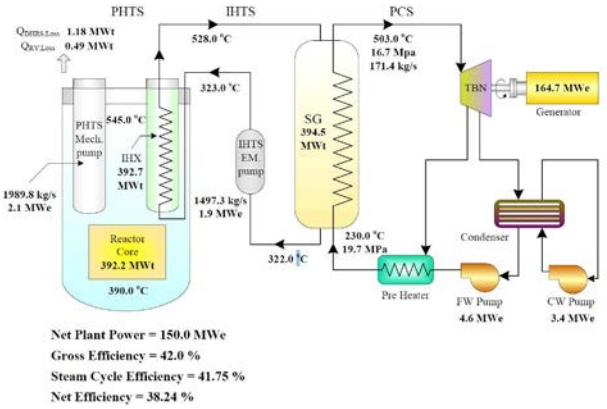

Fig. 3. Heat Balance during 100% Power Operation

development, since the BOP system has no influence on the safety performance of the PGSFR, it was simply modeled as boundary conditions in terms of the feed-water and steam thermodynamic conditions.

2.4 DHRS Models

The decay heat removal system (DHRS) is a designated safety grade system providing a sufficient decay heat removal capability during an abnormal condition, such as a loss of heat sink accident. The DHRS is composed of two passive decay heat removal systems (PDHRS) and two active decay heat removal systems (ADHRS). The PDHRS relies exclusively on a natural convection heat transfer i.e., natural circulation on the sodium side and natural draft on the air side. Fig. 4 shows the normal operational condition for the passive and active DHRSs. The PDHRS consist of two independent loops is equipped with one sodium-sodium decay heat exchanger (DHX), one sodium-air heat exchanger (AHX or FHX), and the heat removing sodium loop connecting the DHX with the AHX. The AHX is a helical type air-sodium heat exchanger in the PDHRS, and the FHX is a finned serpentine-type air-sodium heat exchanger in the ADHRS. The DHX extracts heat through the heat transfer capability of the AHX or FHX, which depends on opening area of the damper in the AHX and operation of the blower in the FHX, respectively. Current heat removal capacities are 0.3 MW and 1MW for normal and accident conditions, respectively.

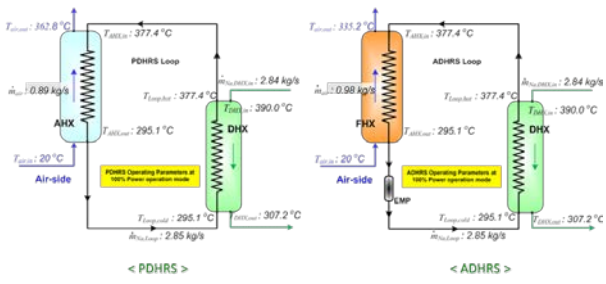

Fig. 4. Normal Conditions for Active and Passive DHRS

2.5 Reactivity Feedback Models

One of major safety mechanisms in an unprotected accident is the reactivity feedback. The MARS code initially has reactivity feedback models, which are similar to the RELAP4 [3]. It is called a separable model, because each effect is assumed to be independent of the other effects. Also, the definition of the separable model is shown in Eq. (1).

$$\begin{aligned} r(t) = r_0 - r_B + \sum_{i=1}^{n_s} r_{si}(t) + \sum_{i=1}^{n_c} V_{ci}(t) + \\ \sum_{i=1}^{n_\rho} \left[W_{\rho i} \cdot R_\rho \left(\rho_i(t) \right) + a_{Wi} \cdot T_{Wi}(t) \right] + \\ \sum_{i=1}^{n_F} \left[W_{Fi} \cdot R_F \left(T_{Fi}(t) \right) + a_{Fi} \cdot T_{Fi}(t) \right] + \\ \sum_{i=1}^{n_\rho} W_{\rho i} \cdot C_b \cdot 10^6 \cdot B_W + r^A + r^R + r^{CRDL/RV} \end{aligned} \quad (1)$$

Basically, reactivity feedbacks in the sodium cooled fast reactor can be classified into five kinds of reactivity feedback components as follows:

Sodium void reactivity

The sodium void reactivity is modeled in the fifth term in Eq. (1). The temperature coefficient, a_{Wi}, is ignored, because the temperature effect is already included in the density variation term, R_ρ. In other words, the density cannot be changed without a temperature variation, because only a single phase sodium condition is assumed. The void reactivity data are obtained from the Core design team.

Doppler reactivity

The Doppler reactivity is modeled as the sixth term in Eq. (1). Doppler reactivities corresponding to fuel temperatures, $R_F(T_{Fi}(t))$ will be a input for MARS-LMR.

Axial fuel expansion reactivity

The axial expansion in a metallic fuel is much larger than that in a ceramic fuel. The effective density of the fuel is decreased as the fuel is axially expanded, which means a higher possibility of neutrons escaping from the core. The modeled axial expansion reactivity, r^A is defined as Eq. (1).

$$r^A = \sum_i C_i^A \left(1 - \frac{\rho_{Fi}^{t=0}}{\rho_{Fi}^{t=t}} \right) \quad (2)$$

C_i^A is a reactivity at node i and its unit is \$. F_i is a fuel density.

Radial core expansion reactivity

The radial size of the core is governed by the subassembly duct, which are supported by grid plates at the inlet region and load pads at the upper region. If temperature of the core is increased, the structures including grid plates and load pads are expanded. Therefore, the reactivity can be reduced owing to a reduction of the effective density in the core. The radial expansion reactivity is modeled with the following Eq. (3)

$$r^R = C^R \ln \left(1 + W_{LP} \sum_i \frac{N_i^{ring}}{N_{total}^{ring}} \varepsilon_i^{LP} + W_{GP} \varepsilon^{GP} \right) \quad (3)$$

C^R is a radial expansion reactivity and its unit is \$. Subscripts i and j are group number for load pad and grid plates, respectively. The parameters of W and ε are the weighting factor and the strain of a structure, respectively. N_{ring} is a radial ring number included in the i-th group, which represents the radial size of the i-th subassembly group.

CRDL/RV expansion reactivity

The control rod is a part of the upper structures. When the temperature of the upper structures is increased, the control rod is inserted to the core region, and thus a negative reactivity feedback occurs. However, as the temperature of the outer wall of the reactor is increased, and the elevation of the core is lower. Thus, the insertion depth of the control rod lowers, and a positive reactivity feedback occurs, although the control rod is not really withdrawn. The control rod has both positive and negative reactivity feedback effects. Therefore, the reactivity feedback is determined by the difference between the reactor vessel expansion and upper structure expansion. This reactivity feedback is defined as Eq. (4).

$$r^{CRDL/RV} = C^{CRDL/RV} \left(\Delta Z_{CRDL} - \Delta Z_{RV} \right) \quad (4)$$

All reactivity feedback coefficients are evaluated from the core design team as summarized in Table I.

Table I. Summary of Reactivity Worth

Feedback coefficient	BOEC	EOEC
Sodium Density [pcm/K]	-0.37651	-0.33749
Doppler [pcm/K]	$-3839.3T^{-1.34997}$	$-4058.5T^{-1.35152}$
Axial Expansion [pcm/K]	-0.24179	-0.25037
Radial Expansion [pcm/K]	-0.7017	-0.72772
Control Rod worth [pcm]		
Primary	8620	8914
Secondary	2665	2794
Total	11285	11708

3. Sensitivity Test for Reactivity Insertion in UTOP

3.1 Reactivity Insertion Amount

The UTOP event is initiated with a single control rod withdrawal. To describe a phenomena related to the control rod withdrawal, the control rod worth and

withdrawal speed are major parameters. Therefore, sensitivity tests for the reactivity insertion rate and the amount of the insertion are conducted at the BOC condition. The 10 and 20 cents including reference of 30 cents as the inserted reactivity amounts and 60, 45 and 30 seconds including reference of 15 seconds as the insertion rates are selected for test cases.

Fig. 5 indicated that the higher insertion amount increases the net positive reactivity. Therefore, a higher amount of reactivity insertion makes higher power as shown in Fig. 6. The peak power and equilibrium power are highly related to the amount of the inserted reactivity. During UTOP events, one of the important components is the steam generator, because the SG has a major heat removal component in the UTOP event. In this analysis, it is assumed the SG can follow the increased power. As the reactivity insertion amount is increased, the peak clad temperatures is increased due to the power increases as shown in Fig. 7. In this event, all reactivity feedback components show negative feedbacks. The major negative reactivity feedback is the core radial expansion component. The higher inlet and outlet core temperatures enhance the larger core radial expansion.

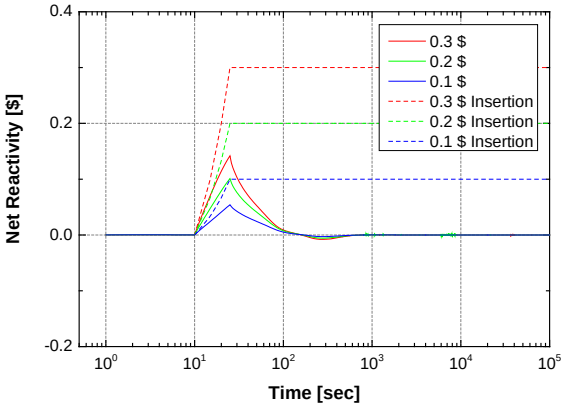

Fig. 5. Net Reactivity for Different Insertion Amounts during UTOP event

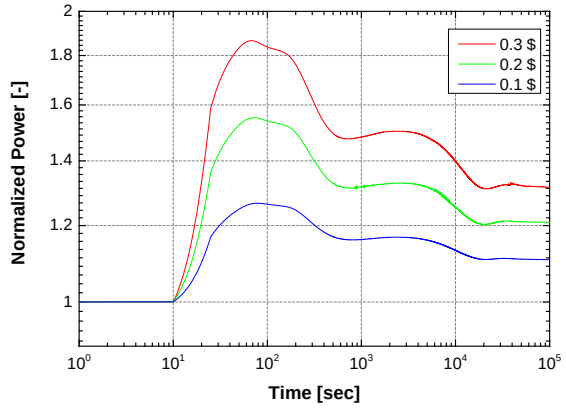

Fig. 6. Normalized Powers with Different Reactivity Insertion Amounts during UTOP Event

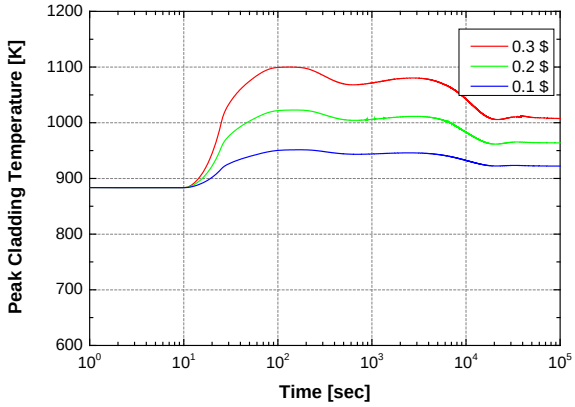

Fig. 7. Peak Clad Temperatures with Different Reactivity Insertion Amount during UTOP Event

3.2 Reactivity Insertion Rates

Fig. 8 indicates that the reactivity insertion rate affects the net reactivity peak. As the insertion rate is slower, the peak net reactivity is reduced. Fig. 9 shows the reactor powers for different reactivity insertion rates during UTOP event. The peak power is slightly reduced as the reactivity insertion rate is smaller, because the peak of the net reactivity is reduced. However, the differences of the peak power are negligible. In addition,

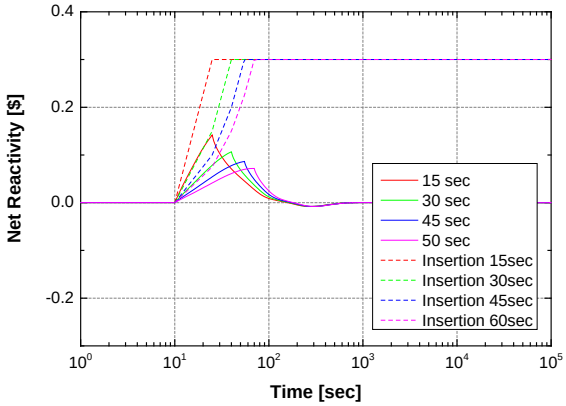

Fig. 8. Net Reactivities with Different Reactivity Insertion Rate during UTOP Event

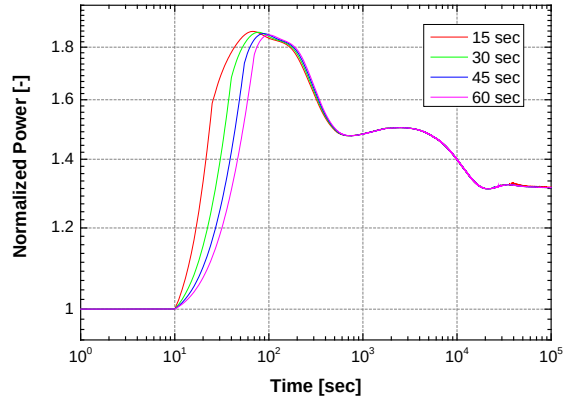

Fig. 9. Normalized Powers with Different Reactivity Insertion Rates during UTOP Event

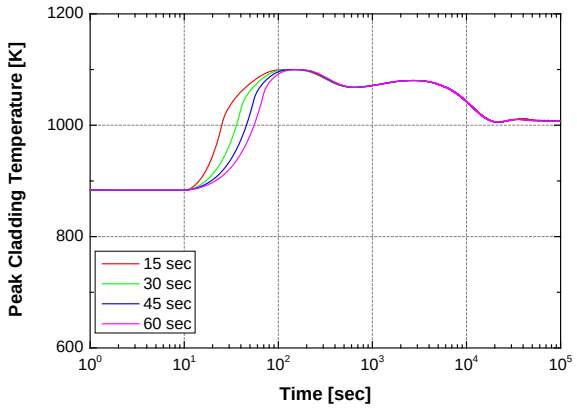

Fig. 10. Peak Clad Temperatures with Different Insertion Rate during UTOP Event

the equilibrium powers are the same with the different insertion rates. It means that a long-term equilibrium power is governed by the only total of amount of reactivity insertion. The peak clad temperatures for different insertion rates are shown in Fig. 10. The insertion rate has influence on only early transient for all phenomena. Reactivity feedbacks show similar trends for all components. Moreover, as the insertion rate slows down, the negative reactivity feedback is decreased.

4. Sensitivity Test of Weighting Factor in Radial Expansion Reactivity Feedback Model

The core radial expansion reactivity is major feedback component during the unprotected events. In the MARS-LMR, the radial reactivity feedback model is defined in Eq. (3). The reference structures for a grid plate and above core load pad are an inlet plenum and subassemblies in the outlet region. Therefore, weighting factors in Eq. (3) means portion of expansion of the grid plate and subassemblies duct in the outlet region. However, there is no physical reasoning or mechanical model. Based on the model in SAS4A/SASSYS code, the weighting factor for the grid plate [4-5], W_{GP} can be evaluated 0.37 as illustrated in Fig. 11. In this model, the weighting factor is defined to evaluate expansion in the mid-plane of the active core. The sensitivity tests of the weighting factors are studied for all unprotected events. The W_{GP} values of 0.1, 0.5, and 0.9 cases are analyzed for the sensitivity test.

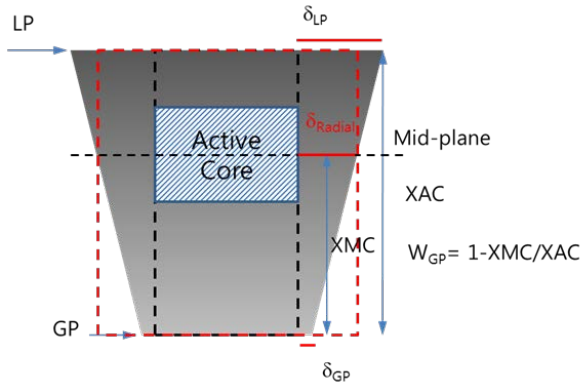

Fig. 11. Schematics for Radial Expansion Model in the SAS4A/SASSYS

4.1 UTOP

Fig. 12 shows normalized powers for different weighting factors in the radial expansion reactivity feedback model. As the weighting factor for the grid plate is increased, the power is increased, which means the contribution of the grid plate in the radial expansion is not predominant. In other words, the inlet temperature rise is smaller than the outlet temperature rise, as shown in Fig. 13. Considering SAS4A/SASSYS's weighting factor, the power shape can be laid between red and green lines. Fig. 14 indicates the net reactivity for different weighting factors. As the W_{GP} is increased, the peak net reactivity is increased, because major contributor of the radial expansion shows smaller negative feedback for a higher W_{GP}. The peak clad temperatures is the same to power trends as shown in Fig. 12.

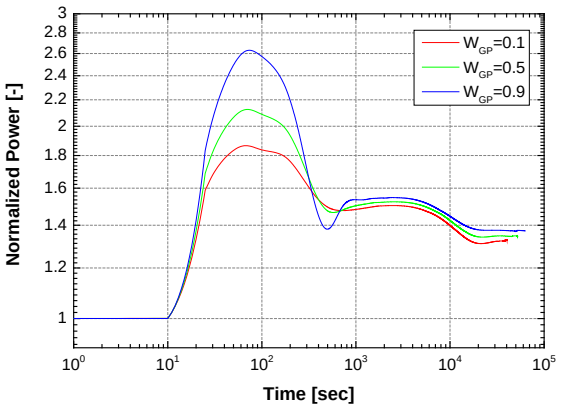

Fig. 12. Normalized Powers with Different Weighting Factors in Core Radial Expansion Reactivity Feedback Model during UTOP Event

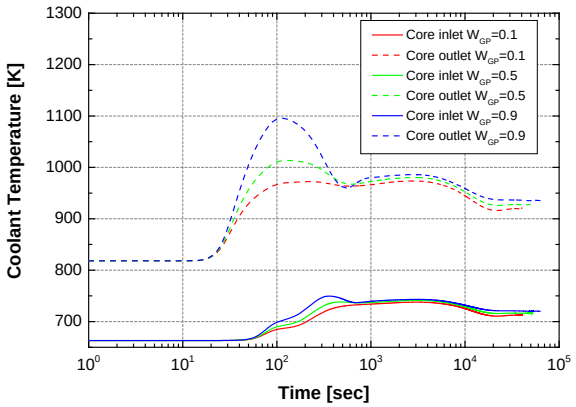

Fig. 13. Core Inlet and Outlet Temperatures with Different Weighting Factors in Core Radial Expansion Reactivity Feedback Model during UTOP Event

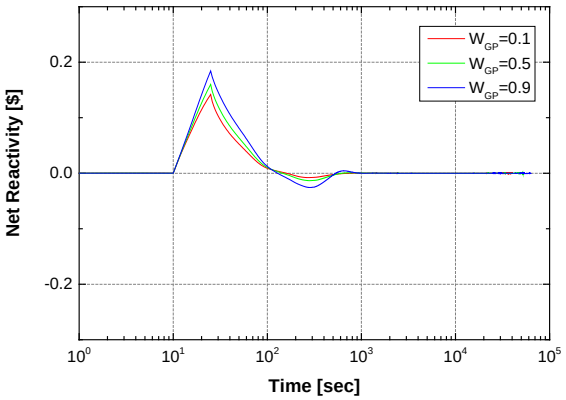

Fig. 14. Reactivity Feedbacks with Different Weighting Factors in Core Radial Expansion Reactivity Feedback Model during UTOP Event

4.2 ULOF

For ULOF events, the weighting factor effect is similar to the UTOP event, since the outlet temperature rise is predominant during this event sequence. Fig. 15 indicates, when the W_{GP} is the higher, the power is higher, because the grid plate temperature rise is much

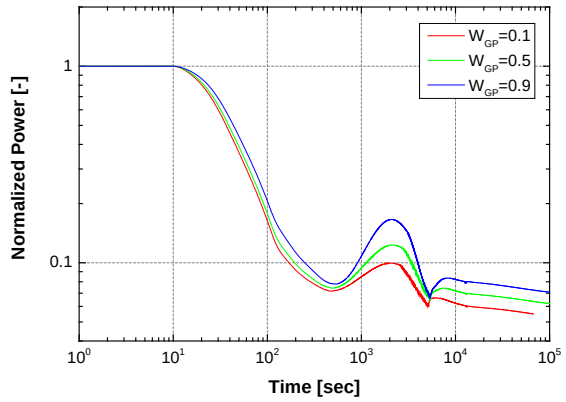

Fig. 15. Normalized Powers with Different Weighting Factors in Core Radial Expansion Reactivity Feedback Model during ULOF Event

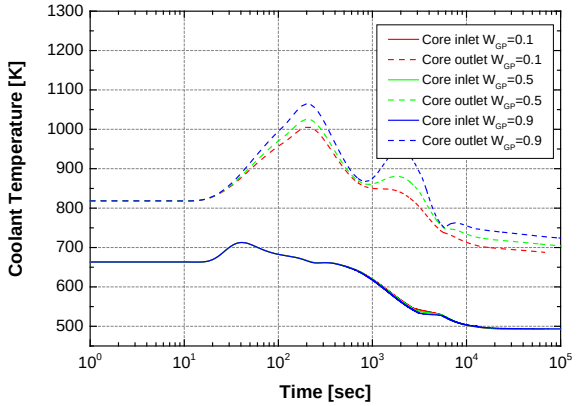

Fig. 16. Core Inlet and Outlet Temperatures with Different Weighting Factors in Core Radial Expansion Reactivity Feedback Model during ULOF Event

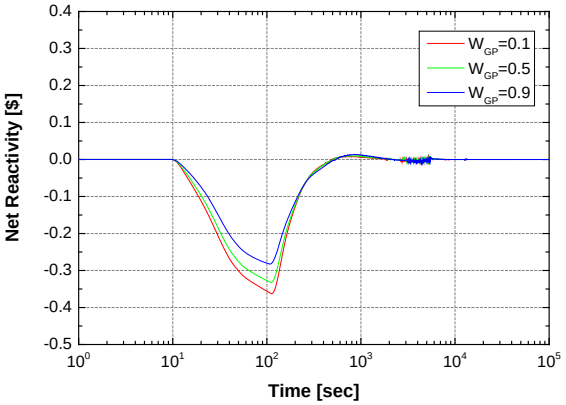

Fig. 17. Reactivity Feedbacks with Different Weighting Factors in Core Radial Expansion Reactivity Feedback Model during ULOF Event

smaller than the load pad (core outlet) temperature rise during the ULOF event (Fig. 16). Therefore, the net negative reactivity for W_{GP} =0.9 is smaller than that in the reference case. In addition, the radial expansion reactivity feedback amount is decreased for a higher weighting factor for the grid plate as shown in Fig. 17. Also, the peak clad temperature is similar to power trends.

4.3 ULOHS

The ULOHS event showed the most severe results among the unprotected events, because the negative reactivity feedback is not enough to shut core down inherently and DHRS capacity. As the W_{GP} is increased, the power is decreased, because the temperature rise in the inlet region (grid plate) is much higher than that in the outlet region (load pad) as shown in Fig. 18 and 19. In ULOHS event, since the primary pumps are still working, the core temperature between inlet and outlet difference is reduced as the reactor power is decreased. Then, the core temperature is continuously rise until the DHRS heat removal balances the reactor power level. When both inlet and outlet coolant temperature are

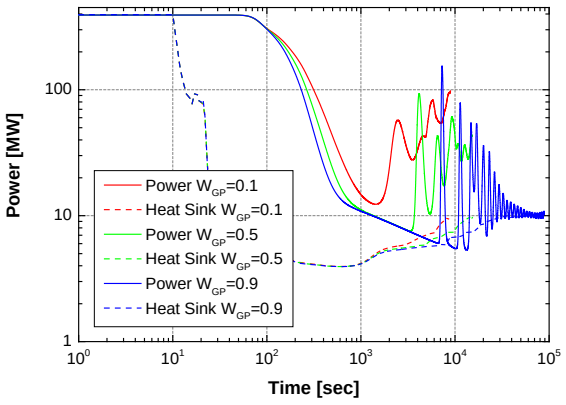

Fig. 18. Reactor Powers and Heat Removal Rates with Different Weighting Factors in Core Radial Expansion Reactivity Feedback Model during ULOHS Event

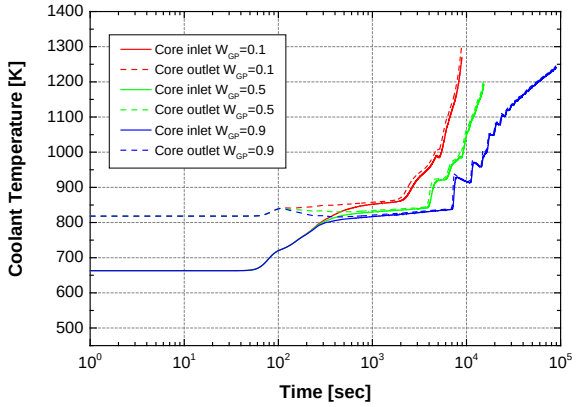

Fig. 19. Core Inlet and Outlet Temperatures with Different Weighting Factors in Core Radial Expansion Reactivity Feedback Model during ULOHS Event

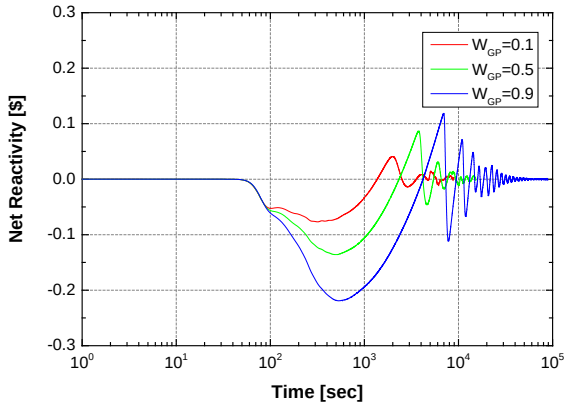

Fig. 20. Reactivity Feedbacks with Different Weighting Factors in Core Radial Expansion Reactivity Feedback Model during ULOHS Event

increased, the reactor vessel expansion is much influential because the cold pool temperature rise is much higher as the same reason of the dependency of the grid plate. Therefore, the only CRDL/RV expansion becomes positive. Simultaneously, the rest of reactivity feedbacks including the radial expansion become negative. These reactivity feedbacks generate a fluctuation of the net reactivity as shown in Fig. 20, which is directly related to the power trends. The peak clad temperature has a similar trend to coolant temperature.

4. Conclusions

The ATWS events for the PGSFR classified in the design extended condition including UTOP, ULOF, and ULOHS are analyzed with MARS-LMR. In this study, the sensitivity tests for reactivity insertion amount and rate in the UTOP event are conducted. The reactivity insertion amount is obviously an influential parameter. The reactivity insertion amount can give a requirement for design of the CRSS, therefore, this sensitivity result is very important to the CRSS. In addition, sensitivity tests for the weighting factor in the radial expansion reactivity model are carried out. The weighting factor for a grid plate, W_{GP}, which means contribution of feedback in the grid plate is changed for all unprotected events. The grid plate expansion is governed by a core inlet temperature. As the W_{GP} is increased, the power in the UTOP and the ULOF is increased, however, the power in the ULOHS is decreased. The higher power during transient means lower reactivity feedback and smaller expansion. Thus, the core outlet temperature rise is dominant in the UTOP and ULOF events, however, the core inlet temperature rise is dominant in the ULOHS. Therefore, the grid plate expansion in the ULOHS is predominant.

These analysis results will give better understanding for the unprotected events and provide feedback to design for the PGSFR. In addition, the safety analyses for unprotected events: UTOP, ULOF, and ULOHS will be recalculated with CDF, which is a safety criteria in the near future. Then, safety margin can be determined quantitatively.

REFERENCES

[1] PRISM Preliminary Safety Information Document (PSID), Appendix E, GEFR-00793 UC-87Ta, 1986.
[2] L. Briggs et. al., Benchmark Analyses of the Shutdown Heat Removal Tests Performed in the EBR-II Reactor, FR13, Paris, France, 4-5 March, 2013
[3] MARS CODE Manual Vol. I: Code Structure, System Models, and Solution Methods, KAERI/TR-2812/2004, Koran Atomic Energy Research and Institute, 2004.
[4] SSC-K Code User Manual Rev.1, KAERI/TR-2014/2002, Koran Atomic Energy Research and Institute, 2002
[5] J. E. Cahalan et. Al., SAS4A-SASSYS-1 Manual: Safety Analysis Code System, Ch4 Reactor Point Kinetics, Decay Heat, and Reactivity Feedback, ANL/NE-12/4, 2012